Title
Novel volumetric method for highly repeatable injection in microchip electrophoresis

Authors
Ha, Noel S
Ly, Jimmy
Jones, Jason
et al.

Publication Date
2017-09-01

DOI
10.1016/j.aca.2017.05.037

Analytica Chimica Acta 985 (2017) 129–140

Contents lists available at ScienceDirect

Analytica Chimica Acta

journal homepage: www.elsevier.com/locate/aca

Novel volumetric method for highly repeatable injection in microchip electrophoresis

Noel S. Ha [a, b], Jimmy Ly [a, b], Jason Jones [b, c], Shilin Cheung [b, 1], R. Michael van Dam [a, b, c, *]

[a] Department of Bioengineering, Henry Samueli School of Engineering and Applied Science, University of California Los Angeles, Los Angeles, CA 90095, USA
[b] Crump Institute for Molecular Imaging and Department of Molecular and Medical Pharmacology, David Geffen School of Medicine, University of California Los Angeles, Los Angeles, CA 90095, USA
[c] Physics & Biology in Medicine Interdepartmental Graduate Program, David Geffen School of Medicine, University of California Los Angeles, Los Angeles, CA 90095, USA

HIGHLIGHTS

- In microchip electrophoresis, there has not been a fixed loop injector as in HPLC to ensure consistent injection volume.
- A novel volumetric injector was developed based on PDMS microvalves.
- Sample injection repeatability is significantly higher than other hydrodynamic and electrokinetic injection methods.
- Consistent injection is achieved, independent of sample constituents and sample viscosity.
- When injector was coupled to a capillary, separation could be achieved with good resolution.

GRAPHICAL ABSTRACT

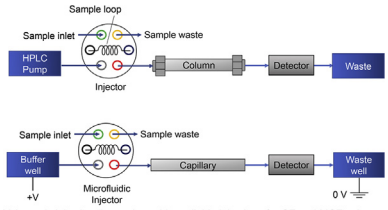

Volumetric injection (bottom) provides reliable injections for CE and MCE using the same concept as an HPLC injection valve (top)

ARTICLE INFO

Article history:
Received 13 April 2017
Received in revised form
22 May 2017
Accepted 22 May 2017
Available online 19 June 2017

Keywords:
Capillary electrophoresis
Sample injection
Injection loop
Volume metering

ABSTRACT

A novel injector for microchip electrophoresis (MCE) has been designed and evaluated that achieves very high repeatability of injection volume suitable for quantitative analysis. It eliminates the injection biases in electrokinetic injection and the dependence on pressure and sample properties in hydrodynamic injection. The microfluidic injector, made of poly(dimethylsiloxane) (PDMS), operates similarly to an HPLC injection valve. It contains a channel segment (chamber) with a well-defined volume that serves as an "injection loop". Using on-chip microvalves, the chamber can be connected to the sample source during the "loading" step, and to the CE separation channel during the "injection" step. Once the valves are opened in the second state, electrophoretic potential is applied to separate the sample. For evaluation and demonstration purposes, the microinjector was connected to a 75 μm ID capillary and UV absorbance detector. For single compounds, a relative standard deviation (RSD) of peak area as low as 1.04% (n = 11) was obtained, and for compound mixtures, RSD as low as 0.40% (n = 4) was observed. Using the

* Corresponding author. California Nanosystems Institute room 4323, 570 Westwood plaza, Los Angeles, CA 90095-7227, USA.
E-mail addresses: noelha@ucla.edu (N.S. Ha), jimmyl81@ucla.edu (J. Ly), jasonjones@mednet.ucla.edu (J. Jones), shilincly@gmail.com (S. Cheung), mvandam@mednet.ucla.edu (R.M. van Dam).
[1] Present address Trace-Ability, Inc., 2446 20th ST #3, Santa Monica, CA, 90405-2716 USA.

http://dx.doi.org/10.1016/j.aca.2017.05.037

Microfluidics
Quality control

same microchip, the performance of this new injection technique was compared to hydrodynamic injection and found to have improved repeatability and less dependence on sample viscosity. Furthermore, a non-radioactive version of the positron-emission tomography (PET) imaging probe, FLT, was successfully separated from its known 3 structurally-similar byproducts with baseline resolution, demonstrating the potential for rapid, quantitative analysis of impurities to ensure the safety of batches of short-lived radiotracers. Both the separation efficiency and injection repeatability were found to be substantially higher when using the novel volumetric injection approach compared to electrokinetic injection (performed in the same chip). This novel microinjector provides a straightforward way to improve the performance of hydrodynamic injection and enables extremely repeatable sample volume injection in MCE. It could be used in any MCE application where volume repeatability is needed, including the quantitation of impurities in pharmaceutical or radiopharmaceutical samples.

1. Introduction

Capillary electrophoresis (CE) is a powerful separation technique with high separation efficiency, flexibility in separation mechanism, low consumption of sample and reagents, and simple instrumentation [1,2]. CE is employed in diverse applications including DNA and protein separation [3–5], detection of disease biomarkers [6,7], environment monitoring on earth and other planets [8,9], food (e.g. wine) analysis [10], and pharmaceutical analysis [11–13]. Unlike other separation methods such as high-performance liquid chromatography (HPLC), CE can more readily be miniaturized using microfluidic chip technology [14–17]. This is especially important for applications where compactness, portability, and/or low cost are needed. Miniaturization confers even further advantages, including lower sample consumption, improved resolution, shorter separation times, improved reproducibility (e.g. from improved temperature control), and increased sensitivity and diversity of detection methods [18–20]. We have previously explored the feasibility of using CE as a replacement for HPLC during quality control (QC) testing of batches of short-lived radioactive positron emission tomography (PET) tracers for medical imaging. With CE, comparable separation performance and limit of detection could be achieved, while analysis times could be shortened in some cases. This is part of a larger effort to miniaturize all stages of tracer production to reduce costs of radiation shielding, equipment, and overall production, which could increase access to diverse PET tracers [21–24].

However, CE has often been considered to have inferior reproducibility compared to other separation techniques such as HPLC or gas chromatography (GC) due to sample injection bias, sample leakage and other factors inherently induced by current sample injection methods, and thus has not been as widely used in quantitative analysis [25–27]. Numerous advances have largely eliminated this concern in recent years [17,28], though achieving the desired degree of reproducibility (e.g. peak area RSD <2% [29]) remains a challenge in many cases. In HPLC, highly repeatable sample volumes are achieved by using “injection valves”. In the “load” state of these specialized two-state valves, a “loop” of well-defined volume is filled with the sample, and, when switched to the “inject” state, this sample is injected directly into the separation pathway. Such method has not been directly applicable to CE due to the much smaller sample volume requirements of CE as well as issues arising from the use of high voltages. However, by developing an electrical decoupler, a similar approach has been shown in conventional, macroscale, CE systems [25,30]. Sample was loaded into a nanoliter-scale injection valve, then pushed via a syringe pump through the electrical decoupler into the separation channel, after which the CE voltage can be applied. Combining this approach with low temperature operation, peak area RSD was reported to be 0.5–2.7%.

In microchip electrophoresis (MCE), however, it is generally preferable that the injection method be integrated directly into the microfluidic chip rather than relying on external systems. Though a wide variety of methods have been explored to increase the reliability of sample injection in MCE [31–33], to the best of our knowledge, there has not been a fixed loop injector as in HPLC that allows the same quantity of sample to be introduced per injection [27]. Typically in MCE devices, injection of sample into a separation channel occurs at the intersection point between a sample channel and the separation channel. The intersection may be a “T”, a cross, a “double T”. With a T junction, the sample flows directly into the separation channel and control of timing or the sample flow determines the injection volume. With a cross or double-T injection, the sample flow crosses the separation channel and flows toward a (sample) waste outlet; the detailed geometry of the junction and operation sequence/timing generally determines the injection volume.

A common way to induce the sample flow is by applying a potential between the sample and a waste well (electrokinetic injection). While very simple and offering the possibility to perform integrated sample concentration (i.e. stacking) [34], this method suffers from injection bias in which solutes with higher electrophoretic mobilities are preferentially introduced, resulting in a difference between the compositions of the original and injected samples [33,35]. The problem is exacerbated with repeated injections, though several groups have developed methods to replenish the sample to mitigate long-term changes in sample composition [36,37]. The electrokinetic injection method is also sensitive to the voltage and to many properties of the sample (e.g. conductivity, pH, possibility of complex formation, electrolysis) [33].

To overcome these drawbacks, pressure-driven injection is becoming more widely used [33]. It is often performed in a cross or double-T geometry by applying a pressure difference between two points to drive sample into the separation channel, and then separation voltage is applied. The resulting sample plug is free of injection bias (thus representative of the original sample). The sample can be driven by hydrostatic pressure [38], with a syringe pump [39], or by applying positive or negative pressure to the sample well [40,41]. A variety of other “plug shaping” techniques have been developed to reduce the sample volume and/or avoid sample “leakage” [39,42], or to improve control of the sample volume [43], but they tend to add complexity and sometimes introduce injection biases.

Despite the advantages of these pressure-driven injection methods, injection reproducibility remains too low in many cases. Rather than rely on geometry to control the injection volume, several methods rely on internal pumps and valves to exert more

precise control over the amount of sample injected. One approach is to use microvalve-based chips [44], typically made from poly(-dimethylsiloxane) (PDMS). The basic concept is to apply constant pressure to the sample and use a computer-controlled microvalve that can be momentarily opened to inject the sample into the separation channel [40,42]. Such valve-based approaches exhibit repeatable sample injection, yielding RSD of the peak area in the range of 1.76–5% [32,45,46]. Though pressure-driven injection eliminates analyte-dependent electrokinetic bias, it could still suffer from other types of variations due to its dependence on flow rate of the sample and microvalve timing to determine the volume injected and could be influenced by the sample properties such as viscosity, which can vary significantly with temperature.

In addition to timing-based valves, other approaches have been developed in an attempt to improve repeatability and reduce dependence on sample properties. Bowen and Martin reported controlling the actuation time and frequency of an on-chip peristaltic pump, rather than timing and pressure, to achieve consistent injection volume [47]. Karlinsey et al. reported a similar approach with a CV of peak area of ~5% [48]. There also has been an attempt to combine the on-chip pump with a valve-enclosed sample loading area; however, it would be challenging to achieve injection repeatability due to problems associated with the large dead volume [49]. Solignac and Gijs reported a different method in which an elastomeric membrane is actuated with an electromagnet to generate a pressure pulse to inject a controllable amount of sample [50]. Though most of these reports did not include reproducibility data, it is expected that all of these methods would still depend on fluid properties similar to hydrodynamic injection.

In this paper we develop a valve-based microchip injection method that eliminates all of these biases and is similar in operation to an HPLC injection valve. Using PDMS microvalves placed around the separation channel, a well-defined fixed volume can be confined within the separation channel in a loading step [51]. Due to the volumetric metering approach, this method eliminates the injection bias found in electrokinetic injection and eliminates the influence of several variables in valve-based injection such as driving pressure, valve response times, or properties of the sample (e.g. viscosity). Furthermore, unlike previously reported methods to meter accurate volumes in an external injection loop, this method is directly integrated into the chip, avoids the need for an electrical decoupler, and avoids dispersion and mixing because the sample does not need to be moved before separation can begin. Thus substantially improved injection repeatability can be expected. We characterize the performance, compare to conventional hydrodynamic injection and electrokinetic injection, and demonstrate the independence from fluid properties such as viscosity.

2. Materials and methods

2.1. Reagents and solutions

Sodium phosphate monobasic (NaH_2PO_4), sodium phosphate dibasic dihydrate (Na_2HPO_4), sodium dodecyl sulfate (SDS), sodium hydroxide (NaOH), 3'-deoxy-3'-fluorothymidine (FLT), thymidine, 2′,3′-didehydro-3′-deoxythymidine (Stavudine) and zidovudine impurity B (chloro-L-thymidine; CLT) were purchased from Sigma Aldrich (Milwaukee, WI, USA). Glycerol (AR® ACS) was purchased from Avantor Performance Materials, Inc. (Center Valley, PA, USA). All chemicals were of analytical grade and were used as received without further purification. Deionized water (18 MΩ) was obtained using a Milli-Q® Integral Water Purification system (EMD Millipore, Billerica, MA, USA).

2.2. Microfluidic chip design and fabrication

The microfluidic injector chip and details of the channel design are shown in Fig. 1. To achieve a well-controlled injection volume, sample is loaded into a fixed-volume chamber within the chip. The chamber is formed from a segment of a microchannel bounded by closed microvalves. The geometry and positioning of the microvalves are designed to minimize the dead volume. Inlets and outlet are connected to the sides of the chamber via microvalves to enable sample loading and washing. Once the chamber has been filled, microvalves at the ends of the chamber are opened, allowing the contents to be injected into the separation channel.

The chip was fabricated in the UCLA Integrated Systems Nanofabrication Cleanroom (ISNC) from poly(dimethylsiloxane) (PDMS) using multilayer soft lithography [44]. The chip consisted of two layers of PDMS bonded to a bottom PDMS substrate layer. Integrated microvalves were formed via a "push-up" valve architecture [52], with valve control channels (15 μm deep x 75 μm wide) molded in the thin PDMS layer closest to the substrate, and fluid-carrying ("flow") channels (20 μm deep x 75 μm wide) molded in a thicker layer above. The flow channel layers had a rounded cross section to enable complete channel sealing when underlying control channels were actuated. To minimize dead volumes, microvalves were placed as close as possible to the edge of the channel they were blocking. Details of the fabrication of molds and microfluidic chips are described in the Supporting Information.

Separation was performed in a 20 cm long, Teflon-coated fused silica capillary (75 μm I.D., 375 μm O.D; Polymicro, Phoenix, AZ, USA) connected to the PDMS chip. In initial experiments, the capillary was connected via a port perpendicular to the channel ("perpendicular junction"). While suitable for characterizing

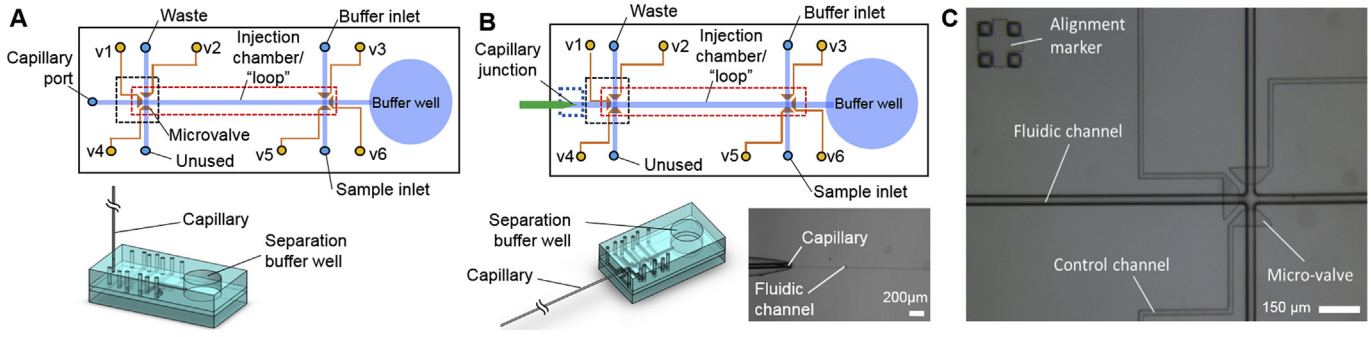

Fig. 1. 3D representation and detailed channel design of the PDMS microfluidic chip connected to a capillary with (A) perpendicular junction geometry and (B) collinear junction geometry. Valve control channels are shown in orange and fluid handling channels are shown in blue. Micrograph of the collinear junction (blue dashed box) is shown in the inset in B. The injection chamber is outlined in a red dashed box. vx = valve control port. (C) Micrograph of the region in the black dashed box. (For interpretation of the references to colour in this figure legend, the reader is referred to the web version of this article.)

volume repeatability, the dead volume inherent in this design led to non-optimal separation. Thus, in later experiments, the capillary was connected by insertion directly into the microchannel through the side of the microfluidic chip ("collinear junction"). The two chip-to-capillary junctions are illustrated in Fig. 1.

2.3. Microchip and capillary conditioning

The chip was hydrated prior to conditioning by filling the chip and capillary with water via the buffer inlet port. Water was loaded at 10 psi for 30 min to ensure all air was purged from the device. The chip was placed in a Petri dish containing a damp Kimwipe and wrapped with parafilm and the other end of the capillary was inserted into a septum-sealed vial containing DI water. Conditioning, to form hydroxyl groups [53] was performed by following this same procedure using 1 M NaOH instead of water. Just prior to use, the NaOH was flushed first with water and then the separation buffer, i.e., 30 mM sodium phosphate buffer with 100 mM SDS.

2.4. Capillary electrophoresis setup

The overall setup to evaluate the PDMS injector chip is shown in Fig. 2. The capillary extending out of the hybrid chip runs through a detection cell and the other end is placed in a PDMS waste well. The waste well is fabricated from two 1″×1/2″ PDMS slabs (~5 mm thick). A well is created by punching a 4.75 mm ID hole through the top slab prior to corona discharge bonding of the two slabs together.

The sample (~1 mL) was contained in a 2 mL septum-sealed vial (Fisherbrand™ 2 mL screw thread autosampler vial, Thermo Fisher Scientific, Waltham, MA, USA). Pressurized nitrogen gas was supplied to the vial through an electronic pressure regulator (ITV0010-3BL, SMC Corporation of America, Noblesville, IN, USA) set to a pressure of 1.5 psi. The vial also contained an outlet tubing (#30 PTFE tubing) connected to the sample inlet port of the injector chip. The buffer was contained in an identical vial, supplied with 6.0 psi nitrogen pressure, and with the outlet tubing connected to the buffer inlet of the injector chip. On-chip microvalves were each controlled by the common port of an external solenoid valve (S070B-5DG, SMC Corporation), connected to the chip via #30 PTFE tubing. The solenoid valves switched between two states: (i) supplying pressurized nitrogen (35 psi) to close the on-chip microvalve, and (ii) venting to atmosphere to allow the on-chip microvalve to open via elastic restoration of the PDMS. To avoid the generation of air bubbles inside the sample-containing channels of the chip, the valve control channels were filled with water. To achieve this, the end of each PTFE tubing was immersed in DI water and a ~1″ water plug aspirated into the tubing prior to connection to the chip. By then supplying 35 psi pressure to each tubing for a few minutes, the small amount of air trapped in the corresponding channel was eliminated prior to operation.

Injected samples were separated via micellular electrokinetic chromatography (MEKC). The separation voltage was provided by a 0–30 kV high voltage DC power supply (HV350, Information Unlimited, Amherst, NH, USA). The tip of the high voltage electrode wire was submerged in the separation buffer well of the injector chip and that of the ground electrode wire was submerged in the PDMS waste well. Electrodes were held in place by electrically-insulated clamps mounted on a retort stand. 4 kV was supplied to achieve a field of 190 V/cm across the separation channel (~1 cm long channel in chip plus 20 cm long capillary). CE voltage was turned on or off using a solid-state relay in series with the high-voltage side of the circuit. During operation, DC current was monitored in real-time via a digital multimeter (Model 2831E, BK precision, Yorba Linda, CA, USA) to detect any abnormal behavior of the chip such as air bubble formation followed by electrical arcing. The typical current was ~0.6 mA. If arcing occurred, the high voltage was immediately interrupted and the channel and capillary were flushed with buffer for 2 min to purge any bubbles and re-equilibrate the inner surfaces.

The detection cell was located 16 cm from the inlet of the capillary, i.e. 17 cm from the point of injection. It consisted of a 4-way junction (PEEK Cross, P-729, Idex Health & Science, Oak Harbor, WA, USA) for aligning the illumination and detection optical fibers with the capillary to perform UV absorbance measurements. Illumination was provided by a deuterium continuous light source (DH2000-DUV, Ocean Optics, Inc, Dunedin, FL, USA) and detection was performed via a spectrometer (USB4000, Ocean Optics, Inc, Dunedin, FL, USA). UV absorbance was measured at 262 nm, corresponding to the wavelength of maximum absorbance for the

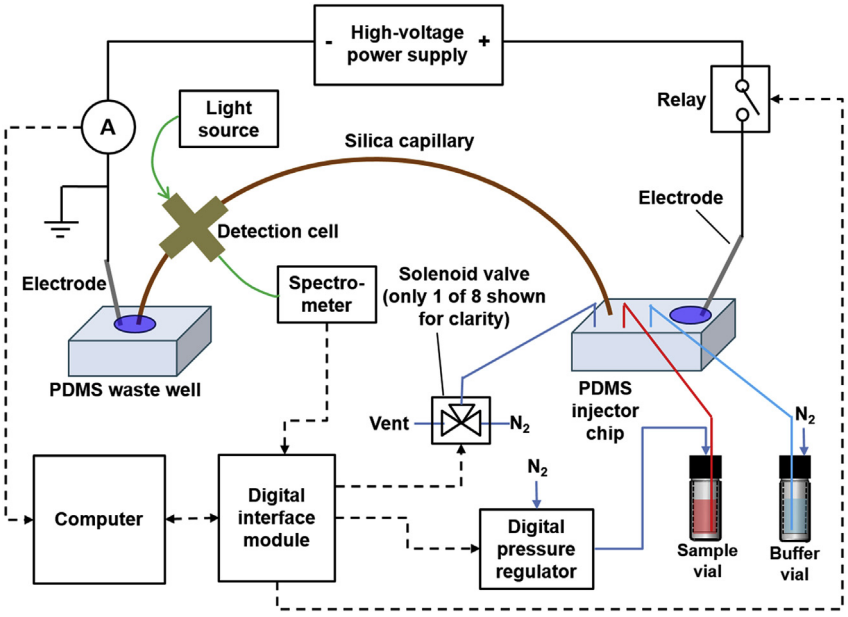

Fig. 2. Experimental setup for evaluation of micro-injector chip.

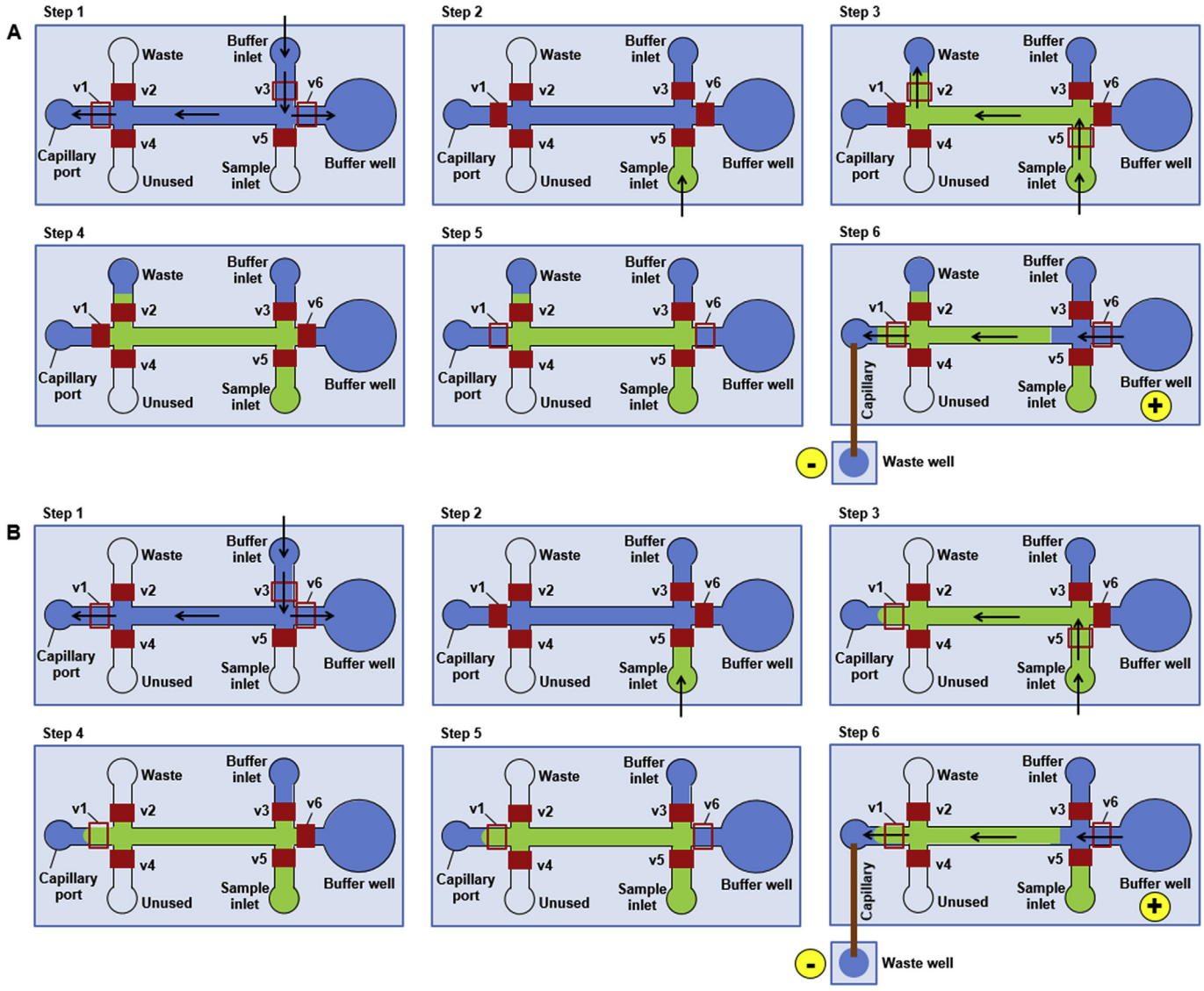

Fig. 3. Schematic view of injector chip operation for volumetric injection (A) and timed injection (B). Solid red boxes indicate closed microvalves and hollow red boxes indicate open microvalves. Arrows indicate direction of fluid flow. Channels filled with buffer are shown in blue while those filled with sample are shown in green. The capillary and waste well are connected for all steps but for clarity are only depicted in the final step when the separation voltage is applied. Diagrams not to scale. (For interpretation of the references to colour in this figure legend, the reader is referred to the web version of this article.)

model compounds used (see Supporting Information).

The solenoid valves, digital pressure regulator and spectrometer were connected to a digital acquisition (DAQ) module (USB 6211, National Instruments Corporation, Austin, TX, USA). A custom-written LabVIEW program (National Instruments Corporation, Austin, TX, USA) was used to coordinate the timing of all functions.

2.5. UV absorbance measurements

Spectrometer output was recorded at a rate of 10 samples/s since the time of injection to create an electropherogram. The transmitted light intensity across the buffer-filled capillary, I_B, was measured by the spectrometer prior to sample injection and used as a reference. Then, the absorbance of the sample (A_S) was calculated as $A_S = \log_{10}(I_S/I_B)$, where I_S is the transmitted light intensity across the capillary containing the sample as measured by the spectrometer.

2.6. Chip operation

2.6.1. Volumetric injection

The detailed steps involved in operation of the chip to perform volumetric injection are shown in Fig. 3A. The basic approach is to prefill a fixed chamber (to volumetrically measure the sample), then open valves to fluidically connect this chamber to the separation channel, and finally apply the electric potential. The chamber was a channel of length 4 mm (75 μm wide, 20 μm deep). Due to the rounded profile the nominal volume is approximately 4 nL. In our chip design, a valve (v7) was also included in the middle of this chamber, enabling switching to a chamber of only half the volume (i.e. ~2 nL). This valve is not shown in Fig. 3A, but is shown in Figure S-2 of the Supporting information. Valve v4 was not used and was kept closed at all times. Before operation, the chip was first primed with buffer (Step 1) to ensure that the tubing from the buffer vial and all channels are filled with buffer. This was accomplished by pressurizing the buffer vial (6 psi) and opening valves v1,

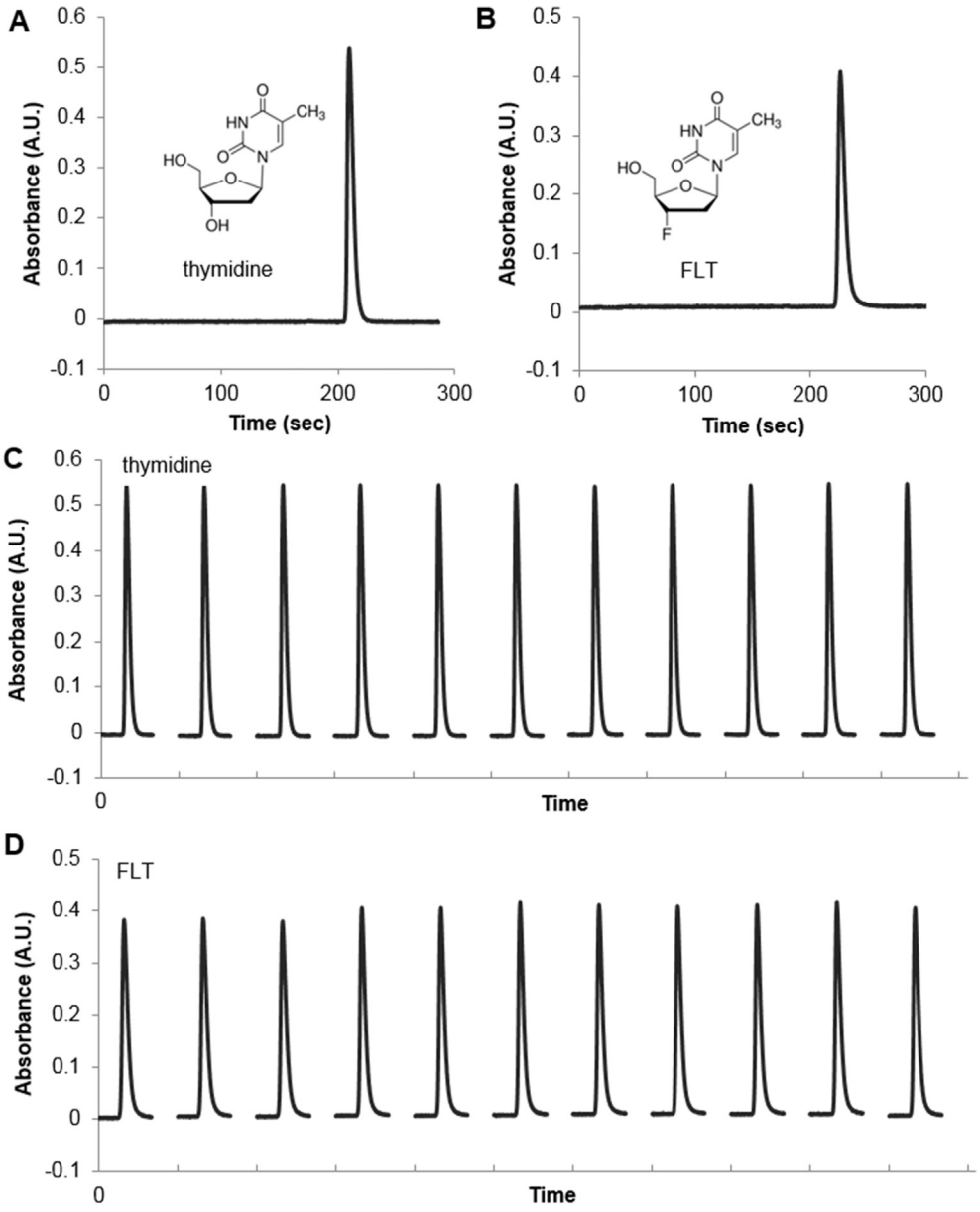

Fig. 4. (A) Example electropherogram of single injection of 50 mM thymidine using the microfluidic volumetric injector chip. (B) Example electropherogram for sample of 50 mM FLT. (C) Assembled electropherograms of successive injections (n = 11) for 50 mM thymidine. Peak area RSD was 1.04%. There is a gap between peaks because the wells were replenished between runs to avoid effects of buffer depletion. (D) Assembled electropherograms for 50 mM FLT. Peak area RSD was 1.55%.

Table 1
Summary of RSD for single-compound injections using volumetric injection and timed injection in the same PDMS chip design. Each RSD value is computed from n = 11 individual injections. A fresh microfluidic chip was used for each trial and for each compound.

Injection method	Injection parameters	Trial	Peak area RSD (%)	
			thymidine	FLT
Volumetric injection	Sample volume = 4 nL	1	1.34	1.79
		2	1.04	1.55
		3	1.47	1.74
Timed injection	Injection time = 600 ms	1	3.37	7.16
		2	4.59	1.86
		3	2.04	3.65

v3, and v6 until the entire channel and capillary were filled with buffer, and the buffer started flowing out of all the ports and buffer well. Next (Step 2), the sample inlet was primed to ensure that the tubing from the sample vial as well as the sample inlet channel were completely filled with sample. This could be accomplished in two ways. In the first method (shown in the figure), the sample vial could be temporarily pressurized to a higher pressure (e.g. ~10 psi) causing the air ahead of the sample to permeate out through the PDMS until the sample inlet was completely filled with sample up to the valve v5 (blind filling). A faster method is to purge the air by applying the normal sample pressure and opening both v2 and v5 until all of the air has passed through v5, the sample chamber, and past v2.

After priming, the sample chamber is loaded by pressurizing the sample to 1.5 psi and opening valves v2 and v5 (Step 3). Once the sample has started exiting the chamber through the waste, v5 is closed first, followed by closure of v2 after a ~2s delay (Step 4). The delay is included so that the sample pressure (1.5 psi) is not "trapped" in the sample chamber, which could distort the PDMS

and change its volume [54]. The sample is then injected by opening valves v1 and v6 (Step 5), allowing a brief delay (150 ms) to ensure the valves are fully open, then applying the electrophoretic potential (Step 6).

Though completion of chamber loading was monitored by observing liquid emerging out of the waste port, which could consume a relatively large amount of sample, it is conceivable to use other means such as on-chip peristaltic pumping for a certain number of cycles [47] to minimize sample consumption associated with each injection.

2.6.2. Timed hydrodynamic injection

Using the same chip, it is also possible to perform conventional hydrodynamic sample injection, providing an ideal benchmark for comparison of the performance of the two injection methods. Basically, the sample is pressurized and a microvalve is momentarily opened to admit a small amount of sample into the separation channel. The detailed operation of the chip to perform "timed injection" is shown in Fig. 3B. Before use, the chip is first primed with buffer (Step 1) by pressurizing the buffer vial and opening valves v1, v3, and v6 until buffer started flow out of all the ports and buffer well. Next, the sample inlet is primed (Step 2) using either of the two methods described in the previous section. If the "purging" method is used, it necessary to flush the sample out of the separation channel by flowing buffer through v3 and v2.

To load the sample, valve v1 is opened, and then valve v5 is momentarily opened for a fixed time to allow sample to fill part of the main channel in the chip (Steps 3–4). The opening time (600 ms) was chosen to achieve a comparable injection volume as the volumetric injection method (see Supporting Information for details). The peak area resulting from volumetric injection was measured to be 3.5 AU-sec and 6.3 AU-sec for the timed injection.To inject the sample, v1 and v6 were opened (Step 5), followed by a brief delay (150 ms), and then electrophoretic potential was applied (Step 6).

It should be noted that in many reports of timed injection, there is no valve interrupting the separation channel. Since the sample flow is less constrained in that case (i.e. it flows both upstream and downstream into the separation channel), we believe such form of timed injection would have comparable or inferior performance to that reported here.

2.7. Injection performance characterization

Using the same chip design, comparisons were made among volumetric injection and timed hydrodynamic injection, as well as electrokinetic injection (see Supporting Information).

Injections were performed with single compounds initially, and then mixtures of multiple compounds. The single-compound samples comprised thymidine in DI water or FLT in 95:5 water:-acetonitrile (v/v). The mixture sample contained thymidine, stavudine, FLT, and CLT in water. These represent the product and structurally-similar side products in the synthesis of the positron emission tomography (PET) tracer [^{18}F]FLT [55,56]. Each injection resulted in an electropherogram. The detected UV absorbance peaks (at 262 nm) were fit to a Gaussian profile to determine the peak area and migration time (t_m; peak center) from each injection. Injection repeatability was measured by performing multiple injections in the same chip and calculating the RSD of peak areas. Sets of injections were performed in different chips to determine consistency.

Since peak symmetry can affect the resolution for mixture samples, we also characterized the peak symmetry by computing the U.S. Pharmacopeia (USP) tailing factor for each peak: $T_f = w_{ac}/2w_{ab}$, where w_{ac} is the peak width at 5% of the peak height, and w_{ab} is the front half-width measured from the leading edge to a perpendicular dropped from the peak apex at 5% of the peak height. Tailing factor close to 1 is desired. The number of theoretical plates was also calculated for each peak: $N = 16 \times (t_m/W)^2$, where t_m is the migration time and W is the baseline peak width determined via the tangent method (see Supporting Information). For mixture samples, the peak resolution between pairs of neighboring peaks was calculated: $R = (t_{m2}-t_{m1})/0.5*(W_1+W_2)$, where t_{mi} is migration time and W_i is the peak width at baseline (tangent method) for each peak ($i = 1,2$).

To avoid effects of buffer depletion, which can affect the migration speed and hence the peak area, the fluidic channels were flushed with fresh buffer solution after each individual injection. In addition, the buffer well and waste well were replenished with ~120 μL each of fresh buffer solution. It may be possible to avoid the need for manual buffer exchange by implmenting wells for buffer and waste that have larger volume. Alternatively, a more sophisticated microfluidic chip could be designed that includes additional valves and pumps to perform automated buffer exchange.

3. Results and discussion

3.1. Comparison of injection performance

In volumetric mode, the microfluidic chip with perpendicular chip-to-capillary junction was used to inject successive ~4 nL samples of single compounds. For each run, the electropherogram showed a flat baseline with a sharp single peak (Fig. 4A,B). The migration time for thymidine was 207 ± 2 s (n = 11), and that for FLT was 221 ± 6 s (n = 11). Examples of the UV absorbance peaks from 11 successive injections in the same chip are shown in Fig. 4C for 50 mM thymidine, and Fig. 4D for 50 mM FLT. Table 1 compares the peak area RSD values. As summarized in Table 1, the peak area RSD values for 3 trials (of 11 injections each) were 1.34%, 1.04%, and 1.47% for thymidine, and 1.79%, 1.55%, and 1.74% for FLT.

The small RSD values are comparable to or better than literature reports. To the best of our knowledge, the best reported peak area RSD was 1.77% (n = 15) using a PDMS chip with integrated microvalves for timed hydrodynamic injection [45]. Since there are many factors of the setup that could affect the apparent consistency of the results (e.g., optical setup, light source stability, detector performance), our results likely cannot be directly compared to those of Li et al.

To better gauge the enhanced performance of volumetric injection, we also performed timed hydrodynamic injection in the same chip to eliminate potential variables. As expected, operation in time-dependent injection mode resulted in higher peak area RSD compared to volumetric injection. For thymidine, we observed peak area RSD values of 2.04%, 3.37% and 4.59% in three chips (11 injections per chip), and for FLT we observed values of 1.86%, 3.65% and 7.16%. Clearly, using the same chip and CE setup, volumetric injection shows significantly improved performance over timed injection.

3.2. Sources of variation in timed injection

We investigated some factors that affect only the timed injection method to see if they could potentially explain the different performance (peak area RSD) between the two injection methods.

One consideration is the stability and repeatability of the pressure source. The flow rate of the sample would be expected to change linearly with any pressure changes. Some reports have controlled pressure via fluid height (hydrostatic pressure) [38,57,58] or external syringe pump [39,59], while we used an electronic pressure regulator. The regulator is reported to have a

stability of ±0.2% of full-scale value (i.e. ±0.06 psi). Since the sample pressure was nominally 1.5 psi, it is possible that pressure fluctuations could be responsible for at least some of the observed variation.

Another consideration is the consistency of microvalve operation: any variation in the opening or closing time could potentially affect the total amount of time the sample is flowing into the separation channel, and thus the volume that is loaded. The actual time the microvalve is open is the programmed opening time minus the opening response time plus the closing response time. The response times depend on several parameters: (i) the pressure of the gas used to control the valves (which may be subject to some fluctuation), (ii) the electromechanical response time of the external solenoid valve that switches between pressurized and vented state, (iii) the fluidic delay due to movement of pneumatic/hydraulic fluid within the valve control channel and valve control line (which would vary based on the amount of hydraulic fluid in the lines), and (iv) the mechanical deflection of the microvalve membrane (which would vary depending on the thickness of the micromachined valve membrane and the elastic properties of the PDMS). By monitoring the electrical current through a microchannel, we found in some cases significant variation (up to several %) in the total open time for a single valve or for different valves in the same chip (see Supporting Information). Variations in amount of hydraulic fluid in the valve control lines seem to have negligible effect on the total open time of the valves (see Supporting Information).

Volumetric injection, on the other hand, provides a way to use similar technology for injection (i.e. microvalves), but eliminate the effect of any variability in driving pressure, valve response times, etc.

3.3. Effect of sample viscosity

The volumetric flow rate, $Q = \Delta p/R$, can be affected by the stability of the driving pressure Δp or by the fluid resistance, R, which is highly dependent on the geometry of the channel as well as fluid properties (i.e., proportional to sample viscosity). A higher viscosity sample will flow more slowly than a low one, so any inconsistencies in sample concentrations, sample buffer composition, or temperature (e.g. Joule heating over time) can lead to poor reproducibility. The latter can be a significant issue as viscosity of aqueous solutions can exhibit significant temperature dependence (e.g., at room temperature, the viscosity of water or saline solution can vary ~2%/°C [60,61]). One of the expected advantages of volumetric injection is that the loaded volume should be independent of the fluid properties. We compared the effect of viscosity on the quantity of sample injected for the two injection methods (Fig. 5). Samples consisted of 50 mM thymidine dissolved in DI water or dissolved in 30% glycerol/water (v/v), with expected dynamic viscosities of 0.893 mPa-s and 2.57 mPa-s, respectively, at room temperature [62,63].

For timed injection, the higher viscosity sample showed significantly lower peak area compared to non-viscous sample ($p = 8 \times 10^{-8} << 0.05$, two-tailed T-test). The peak area was 3.58 ± 0.10 AU-sec (n = 6) for the low viscosity sample and 2.84 ± 0.09 AU-sec (n = 6) for the high viscosity sample. Based on the Hagen-Poiseuille equation, the flow rate is expected to be inversely related to the dynamic viscosity, and so a nearly 3-fold reduction in injected volume would be expected based on the viscosity differences (for the same driving pressure and valve opening time). A smaller reduction was seen, perhaps due in part to the elastic nature of the PDMS which may expand slightly and tend to reduce the fluidic resistance, counteracting the effect of increased viscosity.

In contrast, with volumetric injection, the peak areas of the low and higher viscosity samples were not significantly different (p = 0.20). The lower viscosity sample had peak area of 3.05 ± 0.08 AU-sec (n = 6), while the higher viscosity sample had peak area of 3.10 ± 0.05 AU-sec (n = 6). Thus the volumetric injection technique is expected to prevent differences in injection amounts for different samples, or for the same sample at different temperatures. This

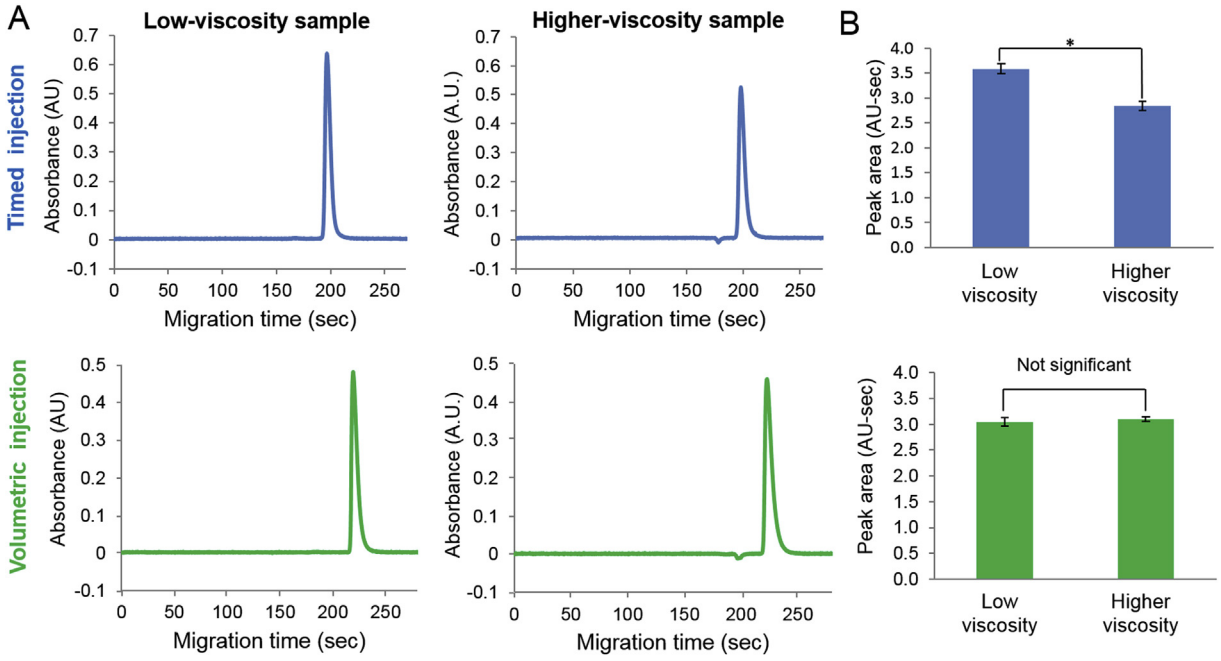

Fig. 5. (A) Representative electropherograms of thymidine samples with different viscosities injected via timed injection (hydrodynamic injection) and volumetric injection. Note that the small negative peak in the eletropherograms for the higher viscosity samples likely represents the glycerol that is present in these samples. (B) Averaged peak area (n = 6 each) observed at detector after separation voltage applied. The use of timed injection results in variation in peak area (i.e. amount injected) depending on viscosity. For volumetric injection, the peak area is independent of viscosity.

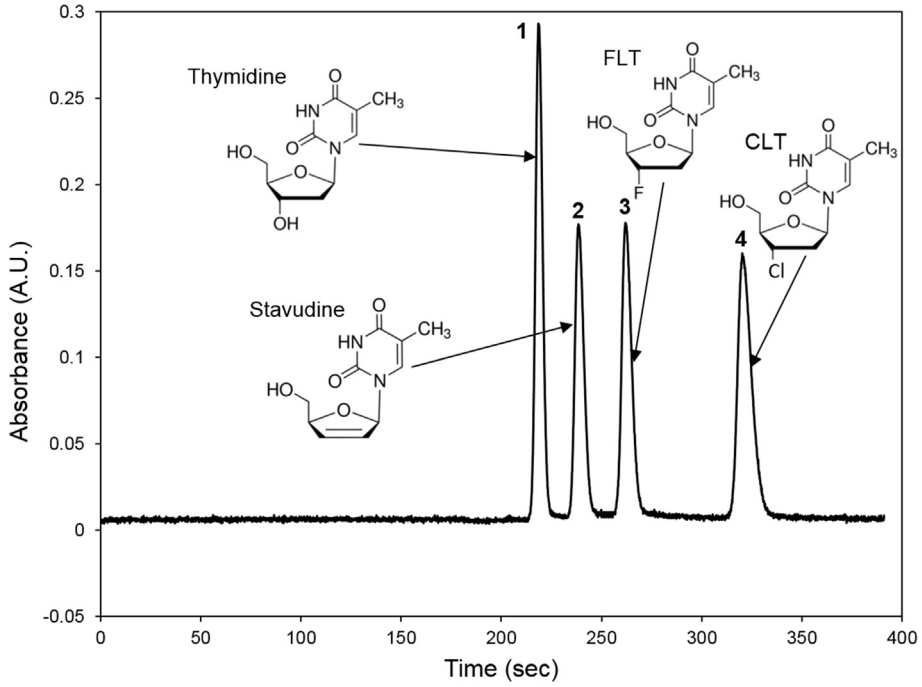

Fig. 6. CE electropherogram showing baseline separation of a mixture of 4 compounds using the microfluidic volumetric injector chip and 20 cm capillary connected via collinear junction. Injected sample contained: 20 mM thymidine (peak 1), 13.6 mM Stavudine (peak 2), 16 mM FLT (peak 3) and 14 mM CLT (peak 4).

could enhance quantitative performance in situations where a variety of different samples (or sample buffers) may be injected in sequence.

3.4. Other comparisons between injection methods

An advantage of timed injection is that different injection volumes can easily be achieved via control of the valve opening time. This flexibility can be used to accommodate different length capillaries or other variations in CE method that might require different sample amounts. In the volumetric approach, the volume too can be adjusted, but requires redesign of the chip to implement a chamber of different volume. Alternatively, modest changes in volume could be achieved by filling the chamber under pressurized conditions, which leads to a predictable expansion of the chamber volume [54]. (The loading process would need to be slightly modified to ensure that the sample chamber is closed while still under pressurized conditions.) Another possible approach to add volume flexibility is to introduce several microvalves along the sample chamber to allow the length of the chamber to be dynamically adjusted (in discrete steps) [64], as was done in the chip designed in this study (i.e. either ~2 or ~4 nL injection volume; see Supporting Information, Figure S-2).

Another difference between the two injection methods is the flow profile. The hydrodynamic flow associated with timed injection has a parabolic velocity profile (i.e. faster flow in middle of channel compared to flow near the walls), which could lead to a small amount of dispersion in the sample plug as it is loaded from the inlet into the separation channel. In contrast, in volumetric injection, the injection chamber is part of the separation pathway and the sample does not undergo this dispersive flow prior to experiencing the separation potential.

3.5. Improvement of peak symmetry

It was evident from the electropherograms (e.g. Fig. 4) that there was significant peak tailing for both the volumetric and timed injection approaches. For samples of 50 mM FLT, the tailing factors were 1.78 ± 0.2 (n = 8; volumetric injection) and 1.80 ± 0.19 (n = 8; timed injection), and for 50 mM thymidine, the tailing factors were 1.62 ± 0.14 (n = 8; volumetric injection) and 1.85 ± 0.05 (n = 8; timed injection).

We suspected the tailing was largely due to the chip-to-capillary junction. The “perpendicular” junction used in initial studies has significant dead volume (see Supporting Information), which is known to be a cause of dispersion and potentially peak asymmetry as the sample plug is flowing through that region [65,66]. To attempt to resolve the issue of peak shape, we implemented an improved chip-to-capillary junction with minimal dead volume. Indeed, when switching to a “collinear” junction geometry, we observed that absorbance peaks were significantly narrower and more symmetric (see Supporting Information, Figure S-11). For samples of 50 mM thymidine, the tailing factor was within the acceptable range (i.e., 1.15 ± 0.01, n = 8) with the collinear junction compared to 1.62 ± 0.14 (n = 8) with the perpendicular junction and this was comparable to the tailing factor of electrokinetic injection with the collinear junction, 1.18 ± 0.21 (n = 8).

In addition, the number of theoretical plates increased from 7770 ± 730 (n = 8) to 9130 ± 710 (n = 8) with use of the collinear junction compared to the perpendicular junction. For a trial of successive injections, the peak area RSD was found to be 1.56% (n = 10), which is in the same range as results with the perpendicular junction chips.

3.6. Separation of 4-compound mixtures

We then examined the ability to separate multiple compounds, and compared results of volumetric injection (with two different junction geometries) as well as the widely-used approach of electrokinetic injection. To avoid introducing additional variables, similar injection volume was used in all three different injection modes (see Supporting Information). Baseline separation of a

Table 2
Summary of peak area RSD (%) for mixture samples.

	Volumetric injection		Electrokinetic injection
	Perpendicular junction (n = 4)	Collinear junction (n = 3)	Collinear junction (n = 3)
thymidine	0.40	0.55	7.13
stavudine	1.59	1.70	7.86
FLT	1.78	0.65	7.79
CLT	1.93	1.69	5.78

Table 3
Summary of the number of theoretical plates and the peak resolution for mixture samples.

	Peak(s)	Volumetric injection		Electrokinetic injection
		Perpendicular junction (n = 4)	Collinear junction (n = 3)	Collinear junction (n = 3)
Number of theoretical plates, N	thymidine	12090 ± 1600	21910 ± 1100	12440 ± 860
	Stavudine	12130 ± 660	18190 ± 550	10720 ± 940
	FLT	10190 ± 750	15390 ± 770	8800 ± 1400
	CLT	14400 ± 1300	17570 ± 1030	8040 ± 530
Peak resolution, R	thymidine-Stavudine	3.18 ± 0.22	3.60 ± 0.19	2.65 ± 0.10
	Stavudine-FLT	2.28 ± 0.09	2.34 ± 0.07	1.77 ± 0.12
	FTL-CLT	7.77 ± 0.44	8.10 ± 0.19	5.32 ± 0.30

mixture of 4 compounds was achieved using the microfluidic volumetric injector chip with the collinear junction (Fig. 6). Separation using the perpendicular junction is shown in the Supporting Information, Figure S-12, and separation using electrokinetic injection is shown in the Supporting Information, Figure S-13.

Peak area RSD values for the 4 compounds and various injection methods are summarized in Table 2. It can be seen that the capillary-to-chip junction geometry does not significantly affect the sample injection repeatability. This is expected because the injected sample amount is physically metered within the injection chamber before even seeing the junction. For volumetric injection, the peak area RSD was always <2.0% and values as low as 0.55% were observed. When electrokinetic injection was performed in the same chip with the same injection volume (as verified by comparing peak areas), the peak area RSD was found to be substantially higher, indicating less consistent sample injection. From these results and the comparison of volumetric and timed injection presented earlier, it appears that sample injection repeatability is mainly influenced by the injection method.

The number of theoretical plates, N, was also calculated for each peak for each junction geometry (Table 3). As expected, we observed N to be significantly higher for all compounds for injection using the collinear junction compared to the perpendicular junction ($p < 0.05$, See Supporting Information for details). In addition, N was significantly higher using volumetric injection than electrokinetic injection in the same chip ($p < 0.05$). The peak resolution, R, was also calculated between pairs of adjacent peaks (Table 3). Peak resolution between the thymidine and Stavudine peaks was significantly higher for volumetric injection using the collinear capillary-to-chip junction compared to the perpendicular junction; however, the difference in resolution for Stavudine and FLT peaks, and for FLT and CLT peaks, was not statistically significant. Interestingly, R was significantly higher for volumetric injection than for electrokinetic injection in the same chip. These results illustrate that the improved injection repeatability does not come at the expense of sacrificed performance elsewhere.

4. Conclusions

A novel type of volumetric microfluidic injector for CE was developed to eliminate variations in injection volume and thereby increase repeatability for quantitative analysis. With this injection method, substantially improved repeatability of sample injection was achieved compared to hydrodynamic injection. Volumetric injection showed relative standard deviation (RSD) of peak area as low as 1.04% (n = 11) for single-compound injections and as low as 0.40% (n = 4) for multiple compound injections, both of which are lower than the best RSD values reported in the literature for hydrodynamic microvalve-based injection. Furthermore, in contrast to hydrodynamic injection, volumetric injection was found not to depend on sample viscosity, which might be beneficial in situations where diverse samples are studied, or where sample temperature is not well controlled.

As a demonstration of the performance of the volumetric injection approach, we showed successful baseline separation of a 4-compound mixture with high injection repeatability. The set of compounds represents a positron emission tomography tracer and synthesis byproducts, illustrating how rapid CE analysis could be used in the QC testing process of radiopharmaceuticals to ensure that levels of impurities are below acceptable limits. In previous work we showed that adequate limit of detection could be achieved for this application [56].

We also made comparisons of injection repeatability, peak symmetry, and separation efficiency for different chip-to-capillary junction geometries between the PDMS injection chip and separation capillary. Injection repeatability was not influenced by the junction geometry, but number of theoretical plates and peak symmetry were all higher in the collinear junction (with very small dead volume) compared to the perpendicular junction (with significant dead volume). Compared to electrokinetic injection (performed in the same chip to avoid introducing additional variables), we found volumetric injection to have significantly higher separation efficiency, resolution, and injection repeatability.

The injector is straightforward to implement with standard PDMS microfluidic fabrication techniques. To increase volume flexibility, valve-based approaches where the volume or length of the chamber is dynamically adjusted can be readily incorporated [54,64]. The separation channel can be incorporated in a hybrid fashion as was done here (i.e. with capillary), or could be integrated directly into the microfluidic chip. This injector would be useful in a

wide range of applications where an accurate and/or consistent injection amount is needed.

Acknowledgments

This work was supported in part by the Department of Energy Office of Biological and Environmental Research (DE-SC0001249) and the National Institute on Aging (R21AG049918).

Appendix A. Supplementary data

Supplementary data related to this article can be found at http://dx.doi.org/10.1016/j.aca.2017.05.037.

References

[1] E. González-Peñas, C. Leache, A. López de Cerain, E. Lizarraga, Comparison between capillary electrophoresis and HPLC-FL for ochratoxin A quantification in wine, Food Chem. 97 (2006) 349–354, http://dx.doi.org/10.1016/j.foodchem.2005.05.007.
[2] T. Faller, H. Engelhardt, How to achieve higher repeatability and reproducibility in capillary electrophoresis, J. Chromatogr. A 853 (1999) 83–94, http://dx.doi.org/10.1016/S0021-9673(99)00382-9.
[3] G.G. Mironov, C.M. Clouthier, A. Akbar, J.W. Keillor, M.V. Berezovski, Simultaneous analysis of enzyme structure and activity by kinetic capillary electrophoresis-MS, Nat. Chem. Biol. Adv. online Publ. (2016), http://dx.doi.org/10.1038/nchembio.2170.
[4] G.G. Morbioli, T. Mazzu-Nascimento, A. Aquino, C. Cervantes, E. Carrilho, Recombinant drugs-on-a-chip: the usage of capillary electrophoresis and trends in miniaturized systems – a review, Anal. Chim. Acta 935 (2016) 44–57, http://dx.doi.org/10.1016/j.aca.2016.06.019.
[5] B.C. Durney, C.L. Crihfield, L.A. Holland, Capillary electrophoresis applied to DNA: determining and harnessing sequence and structure to advance bioanalyses (2009–2014), Anal. Bioanal. Chem. 407 (2015) 6923–6938, http://dx.doi.org/10.1007/s00216-015-8703-5.
[6] Z. Yang, J.V. Sweedler, Application of capillary electrophoresis for the early diagnosis of cancer, Anal. Bioanal. Chem. 406 (2014) 4013–4031, http://dx.doi.org/10.1007/s00216-014-7722-y.
[7] A.N. de Macedo, M. Irfan Yasin Jiwa, J. Macri, V. Belostotsky, S. Hill, P. Britz-McKibbin, Strong anion determination in biological fluids by capillary electrophoresis for clinical diagnostics, Anal. Chem. 85 (2013) 11112–11120, http://dx.doi.org/10.1021/ac402975q.
[8] S.-K. Ruokonen, F. Duša, J. Lokajová, I. Kilpeläinen, A.W.T. King, S.K. Wiedmer, Effect of ionic liquids on the interaction between liposomes and common wastewater pollutants investigated by capillary electrophoresis, J. Chromatogr. A 1405 (2015) 178–187, http://dx.doi.org/10.1016/j.chroma.2015.05.064.
[9] A.M. Skelley, J.R. Scherer, A.D. Aubrey, W.H. Grover, R.H.C. Ivester, P. Ehrenfreund, F.J. Grunthaner, J.L. Bada, R.A. Mathies, Development and evaluation of a microdevice for amino acid biomarker detection and analysis on mars, Proc. Natl. Acad. Sci. U. S. A. 102 (2005) 1041–1046, http://dx.doi.org/10.1073/pnas.0406798102.
[10] F.J.V. Gomez, M.F. Silva, Microchip electrophoresis for wine analysis, Anal. Bioanal. Chem. (2016) 1–11, http://dx.doi.org/10.1007/s00216-016-9841-0.
[11] E. Tamizi, A. Jouyban, The potential of the capillary electrophoresis techniques for quality control of biopharmaceuticals—a review, Electrophoresis 36 (2015) 831–858, http://dx.doi.org/10.1002/elps.201400343.
[12] A. Lloyd, M. Russell, L. Blanes, R. Somerville, P. Doble, C. Roux, The application of portable microchip electrophoresis for the screening and comparative analysis of synthetic cathinone seizures, Forensic Sci. Int. 242 (2014) 16–23, http://dx.doi.org/10.1016/j.forsciint.2014.06.013.
[13] L. Suntornsuk, Recent advances of capillary electrophoresis in pharmaceutical analysis, Anal. Bioanal. Chem. 398 (2010) 29–52, http://dx.doi.org/10.1007/s00216-010-3741-5.
[14] E.R. Castro, A. Manz, Present state of microchip electrophoresis: state of the art and routine applications, J. Chromatogr. A 1382 (2015) 66–85, http://dx.doi.org/10.1016/j.chroma.2014.11.034.
[15] D. Janasek, J. Franzke, A. Manz, Scaling and the design of miniaturized chemical-analysis systems, Nature 442 (2006) 374–380, http://dx.doi.org/10.1038/nature05059.
[16] A.P. Lewis, A. Cranny, N.R. Harris, N.G. Green, J.A. Wharton, R.J.K. Wood, K.R. Stokes, Review on the development of truly portable and in-situ capillary electrophoresis systems, Meas. Sci. Technol. 24 (2013) 042001, http://dx.doi.org/10.1088/0957-0233/24/4/042001.
[17] M.C. Breadmore, Capillary and microchip electrophoresis: challenging the common conceptions, J. Chromatogr. A 1221 (2012) 42–55, http://dx.doi.org/10.1016/j.chroma.2011.09.062.
[18] J.V. Pagaduan, V. Sahore, A.T. Woolley, Applications of microfluidics and microchip electrophoresis for potential clinical biomarker analysis, Anal. Bioanal. Chem. 407 (2015) 6911–6922, http://dx.doi.org/10.1007/s00216-015-8622-5.
[19] F. Shang, E. Guihen, J.D. Glennon, Recent advances in miniaturisation—the role of microchip electrophoresis in clinical analysis, Electrophoresis 33 (2012) 105–116, http://dx.doi.org/10.1002/elps.201100454.
[20] S. Ohla, D. Belder, Chip-based separation devices coupled to mass spectrometry, Curr. Opin. Chem. Biol. 16 (2012) 453–459, http://dx.doi.org/10.1016/j.cbpa.2012.05.180.
[21] G. Pascali, L. Matesic, How far are we from dose on demand of short-lived radiopharmaceuticals?, in: Y. Kuge, T. Shiga, N. Tamaki (Eds.), Perspect. Nucl. Med. Mol. Diagn. Integr. Ther, Springer, Japan, 2016, pp. 79–92, http://dx.doi.org/10.1007/978-4-431-55894-1_6.
[22] P.Y. Keng, M. Sergeev, R.M. van Dam, Advantages of radiochemistry in microliter volumes, in: Y. Kuge, T. Shiga, N. Tamaki (Eds.), Perspect. Nucl. Med. Mol. Diagn. Integr. Ther, Springer, Japan, 2016, pp. 93–111, http://dx.doi.org/10.1007/978-4-431-55894-1_7.
[23] W.-Y. Tseng, R.M. van Dam, Compact microfluidic device for rapid concentration of PET tracers, Lab. Chip 14 (2014) 2293, http://dx.doi.org/10.1039/c4lc00286e.
[24] C. Rensch, A. Jackson, S. Lindner, R. Salvamoser, V. Samper, S. Riese, P. Bartenstein, C. Wängler, B. Wängler, Microfluidics: a groundbreaking technology for PET tracer production? Molecules 18 (2013) 7930–7956, http://dx.doi.org/10.3390/molecules18077930.
[25] Y. Xu, B. Ling, W. Zhu, D. Yao, L. Zhang, Y. Wang, C. Yan, Development of fully automated quantitative capillary electrophoresis with high accuracy and repeatability, Biomed. Chromatogr. 30 (2016) 390–395, http://dx.doi.org/10.1002/bmc.3560.
[26] B.X. Mayer, How to increase precision in capillary electrophoresis, J. Chromatogr. A 907 (2001) 21–37, http://dx.doi.org/10.1016/S0021-9673(00)01057-8.
[27] J.P. Schaeper, M.J. Sepaniak, Parameters affecting reproducibility in capillary electrophoresis, Electrophoresis 21 (2000) 1421–1429, http://dx.doi.org/10.1002/(SICI)1522-2683(20000401)21, 7<1421::AID-ELPS1421>3.0.CO;2–7.
[28] U. Holzgrabe, D. Brinz, S. Kopec, C. Weber, Y. Bitar, Why not using capillary electrophoresis in drug analysis? Electrophoresis 27 (2006) 2283–2292, http://dx.doi.org/10.1002/elps.200600016.
[29] C. Cianciulli, H. Wätzig, Analytical instrument qualification in capillary electrophoresis, Electrophoresis 33 (2012) 1499–1508, http://dx.doi.org/10.1002/elps.201100699.
[30] M. Li, J. Zhou, X. Gu, Y. Wang, X. Huang, C. Yan, Quantitative capillary electrophoresis and its application in analysis of alkaloids in tea, coffee, coca cola, and theophylline tablets, J. Sep. Sci. 32 (2009) 267–274, http://dx.doi.org/10.1002/jssc.200800529.
[31] B.W. Wenclawiak, R.J. Püschl, Sample injection for capillary electrophoresis on a micro fabricated device/on chip CE injection, Anal. Lett. 39 (2006) 3–16, http://dx.doi.org/10.1080/00032710500460932.
[32] J.M. Karlinsey, Sample introduction techniques for microchip electrophoresis: a review, Anal. Chim. Acta 725 (2012) 1–13, http://dx.doi.org/10.1016/j.aca.2012.02.052.
[33] R.M. Saito, W.K.T. Coltro, D.P. Jesus, Instrumentation design for hydrodynamic sample injection in microchip electrophoresis: a review, Electrophoresis 33 (2012) 2614–2623, http://dx.doi.org/10.1002/elps.201200089.
[34] M.C. Breadmore, A.I. Shallan, H.R. Rabanes, D. Gstoettenmayr, A.S. Abdul Keyon, A. Gaspar, M. Dawod, J.P. Quirino, Recent advances in enhancing the sensitivity of electrophoresis and electrochromatography in capillaries and microchips (2010–2012), Electrophoresis 34 (2013) 29–54, http://dx.doi.org/10.1002/elps.201200396.
[35] J.P. Landers, Handbook of Capillary Electrophoresis, second ed., CRC Press, 1996.
[36] Q. Fang, F.-R. Wang, S.-L. Wang, S.-S. Liu, S.-K. Xu, Z.-L. Fang, Sequential injection sample introduction microfluidic-chip based capillary electrophoresis system, Anal. Chim. Acta 390 (1999) 27–37, http://dx.doi.org/10.1016/S0003-2670(99)00183-X.
[37] P. Kuban, K. Tennberg, R. Tryzell, B. Karlberg, Calibration principles for flow injection analysis–capillary electrophoresis systems with electrokinetic injection, J. Chromatogr. A 808 (1998) 219–227, http://dx.doi.org/10.1016/S0021-9673(98)00130-7.
[38] Y. Luo, D. Wu, S. Zeng, H. Gai, Z. Long, Z. Shen, Z. Dai, J. Qin, B. Lin, Double-cross hydrostatic pressure sample injection for chip CE: variable sample plug volume and minimum number of electrodes, Anal. Chem. 78 (2006) 6074–6080, http://dx.doi.org/10.1021/ac0605142.
[39] N. Dossi, R. Toniolo, S. Susmel, A. Pizzariello, G. Bontempelli, A simple approach to the hydrodynamic injection in microchip electrophoresis with electrochemical detection, Electrophoresis 31 (2010) 2541–2547, http://dx.doi.org/10.1002/elps.201000089.
[40] R.T. Kelly, C. Wang, S.J. Rausch, C.S. Lee, K. Tang, Pneumatic microvalve-based hydrodynamic sample injection for high-throughput, quantitative zone electrophoresis in capillaries, Anal. Chem. 86 (2014) 6723–6729, http://dx.doi.org/10.1021/ac501910p.
[41] X. Sun, R.T. Kelly, W.F. Danielson, N. Agrawal, K. Tang, R.D. Smith, Hydrodynamic injection with pneumatic valving for microchip electrophoresis with total analyte utilization, Electrophoresis 32 (2011) 1610–1618, http://dx.doi.org/10.1002/elps.201000522.
[42] Y. Cong, S. Katipamula, T. Geng, S.A. Prost, K. Tang, R.T. Kelly, Electrokinetic sample preconcentration and hydrodynamic sample injection for microchip electrophoresis using a pneumatic microvalve, Electrophoresis 37 (2016)

455–462, http://dx.doi.org/10.1002/elps.201500286.
[43] A. Gáspár, P.I. Koczka, H. Carmona, F.A. Gomez, Split injection: a simple introduction of subnanoliter sample volumes for chip electrophoresis, Microchem. J. 99 (2011) 180–185, http://dx.doi.org/10.1016/j.microc.2011.05.001.
[44] M.A. Unger, H.-P. Chou, T. Thorsen, A. Scherer, S.R. Quake, Monolithic microfabricated valves and pumps by multilayer soft lithography, Science 288 (2000) 113–116, http://dx.doi.org/10.1126/science.288.5463.113.
[45] M.W. Li, B.H. Huynh, M.K. Hulvey, S.M. Lunte, R.S. Martin, Design and characterization of poly(dimethylsiloxane)-based valves for interfacing continuous-flow sampling to microchip electrophoresis, Anal. Chem. 78 (2006) 1042–1051, http://dx.doi.org/10.1021/ac051592c.
[46] A.K. Price, C.T. Culbertson, Generation of nonbiased hydrodynamic injections on microfluidic devices using integrated dielectric elastomer actuators, Anal. Chem. 81 (2009) 8942–8948, http://dx.doi.org/10.1021/ac9015837.
[47] A.L. Bowen, R.S. Martin, Integration of on-chip peristaltic pumps and injection valves with microchip electrophoresis and electrochemical detection, Electrophoresis 31 (2010) 2534–2540, http://dx.doi.org/10.1002/elps.201000029.
[48] J.M. Karlinsey, J. Monahan, D.J. Marchiarullo, J.P. Ferrance, J.P. Landers, Pressure injection on a valved microdevice for electrophoretic analysis of submicroliter samples, Anal. Chem. 77 (2005) 3637–3643, http://dx.doi.org/10.1021/ac048115z.
[49] V. Sahore, S. Kumar, C.I. Rogers, J.K. Jensen, M. Sonker, A.T. Woolley, Pressure-actuated microfluidic devices for electrophoretic separation of pre-term birth biomarkers, Anal. Bioanal. Chem. 408 (2015) 599–607, http://dx.doi.org/10.1007/s00216-015-9141-0.
[50] D. Solignac, M.A.M. Gijs, Pressure pulse Injection: a powerful alternative to electrokinetic sample loading in electrophoresis microchips, Anal. Chem. 75 (2003) 1652–1657, http://dx.doi.org/10.1021/ac026350g.
[51] B.T.C. Lau, C.A. Baitz, X.P. Dong, C.L. Hansen, A complete microfluidic screening platform for rational protein crystallization, J. Am. Chem. Soc. 129 (2007) 454–455, http://dx.doi.org/10.1021/ja065855b.
[52] V. Studer, G. Hang, A. Pandolfi, M. Ortiz, W.F. Anderson, S.R. Quake, Scaling properties of a low-actuation pressure microfluidic valve, J. Appl. Phys. 95 (2004) 393–398, http://dx.doi.org/10.1063/1.1629781.
[53] I. Hoek, F. Tho, W.M. Arnold, Sodium hydroxide treatment of PDMS based microfluidic devices, Lab. Chip 10 (2010) 2283, http://dx.doi.org/10.1039/c004769d.
[54] K. Liu, Y.-C. Chen, H.-R. Tseng, C.K.-F. Shen, R.M. van Dam, Microfluidic device for robust generation of two-component liquid-in-air slugs with individually controlled composition, Microfluid. Nanofluidics 9 (2010) 933–943, http://dx.doi.org/10.1007/s10404-010-0617-0.
[55] C. Pascali, A. Bogni, L. Fugazza, C. Cucchi, O. Crispu, L. Laera, R. Iwata, G. Maiocchi, F. Crippa, E. Bombardieri, Simple preparation and purification of ethanol-free solutions of 3′-deoxy-3′-[18F]fluorothymidine by means of disposable solid-phase extraction cartridges, Nucl. Med. Biol. 39 (2012) 540–550, http://dx.doi.org/10.1016/j.nucmedbio.2011.10.005.
[56] S. Cheung, J. Ly, M. Lazari, S. Sadeghi, P.Y. Keng, R.M. van Dam, The separation and detection of PET tracers via capillary electrophoresis for chemical identity and purity analysis, J. Pharm. Biomed. Anal. 94 (2014) 12–18, http://dx.doi.org/10.1016/j.jpba.2014.01.023.
[57] H. Gai, L. Yu, Z. Dai, Y. Ma, B. Lin, Injection by hydrostatic pressure in conjunction with electrokinetic force on a microfluidic chip, Electrophoresis 25 (2004) 1888–1894, http://dx.doi.org/10.1002/elps.200305835.
[58] X. Huang, M.J. Gordon, R.N. Zare, Bias in quantitative capillary zone electrophoresis caused by electrokinetic sample injection, Anal. Chem. 60 (1988) 375–377, http://dx.doi.org/10.1021/ac00155a023.
[59] C.-C. Lin, C.-C. Chen, C.-E. Lin, S.-H. Chen, Microchip electrophoresis with hydrodynamic injection and waste-removing function for quantitative analysis, J. Chromatogr. A 1051 (2004) 69–74, http://dx.doi.org/10.1016/j.chroma.2004.08.040.
[60] J. Kestin, I.R. Shankland, Viscosity of aqueous NaCl solutions in the temperature range 25–200°C and in the pressure range 0.1–30 MPa, Int. J. Thermophys. 5 (n.d.) 241–263. doi:10.1007/BF00507835.
[61] J. Kestin, M. Sokolov, W.A. Wakeham, Viscosity of liquid water in the range −8°C to 150°C, J. Phys. Chem. Ref. Data 7 (1978) 941–948, http://dx.doi.org/10.1063/1.555581.
[62] P.N. Shankar, M. Kumar, Experimental determination of the kinematic viscosity of glycerol-water mixtures, Proc. R. Soc. Lond. Math. Phys. Eng. Sci. 444 (1994) 573–581, http://dx.doi.org/10.1098/rspa.1994.0039.
[63] N.-S. Cheng, Formula for the viscosity of a Glycerol–Water mixture, Ind. Eng. Chem. Res. 47 (2008) 3285–3288, http://dx.doi.org/10.1021/ie071349z.
[64] Y.-C. Chen, K. Liu, C.K.-F. Shen, R.M. van Dam, On-demand generation and mixing of liquid-in-gas slugs with digitally programmable composition and size, J. Micromechanics Microengineering 25 (2015) 084006, http://dx.doi.org/10.1088/0960-1317/25/8/084006.
[65] N.H. Bings, C. Wang, C.D. Skinner, C.L. Colyer, P. Thibault, D.J. Harrison, Microfluidic devices connected to fused-silica capillaries with minimal dead volume, Anal. Chem. 71 (1999) 3292–3296.
[66] C.-H. Chiou, G.-B. Lee, Minimal dead-volume connectors for microfluidics using PDMS casting techniques, J. Micromechanics Microengineering 14 (2004) 1484.